Ferrohydrodynamic of a Rotating Disk with Vertical Motion

P.Gayathri[1], N. Nithyadevi[2], M. Gowri[2]&C. Udhaya Shankar[3]

[1]Department of Mathematics, PSG College of Arts and Science, India
[2]Department of Mathematics, Bharathiar University, India
[3]Department of Electrical and Electronics Engineering, SNS College of Engineering, India

Abstract

The numerical investigation of lowly oscillating magneto viscous flow above a non electrically conducting heated rotating disk subject to vertical motion of the disk(both upward and downward movement) is performed. The ferronanoparticles (Fe_3O_4) is incorporated into the fluid flow and the corresponding ferrohydrodynamic equations of motion along with the magnetization equation are framed using Shliomis theory. This pumping flow problem governed by partial differential equations are regenerated as non linear ordinary differenatial equations using von Karman similarity procedure. The computational analysis based on finite difference collocation method was utilized to obtain numerical values of fluid motion components. It was found that the vertical movement of the disk with its parameter shows an increasing velocity and temperature profile. Moreover, the increase of ferrofluid concentration with respect to the magnetization parameter has a positive impact on reduced skin friction along tangential direction and heat transfer coefficient.

Keywords: Ferrofluid, Low Oscillating Magnetic Field, Vertical Disk Motion, Mixed Convection.

1. Introduction

An infinite long plane disk subjected to uniform rotation creates a flow named as vonKarman swirling flow whenTheodre von Karman (1921) noticed the fluid motion by the rotating disk which makes the fluid to move outwards because of centrifugal force. The rotating disk is taken as an action of fluid pump and this is used in modeling compressor and centrifugal fans. This study has its own applications in wide range such as filtering systems, heat and mass transfer, rotating machines, computer storage devices, planetary formations, combustion problems, geophysical applications and so many. Millaps and Pohlhausen (1952) made a study on thermal behavior owing to laminar viscous flow adjacebt above the rotating plate. The magnetoviscous flow solutions with the conjugated Hall current effects due to an infinitely rotating disk was determined by Attia and Aboul-Hassan (2004). The viscous momentum layers contoured due to the impact of rigid rotating disks with surface roughness was examined experimentally under different circumstances by Miklavcic and Wang (2004). Arikoglu et al. (2006) investigated the von Karman flow with entropy generation in single rotating disk. Ahmadpour and Sadeghy (2013) revealed the existence of the exact solutions of the exact solution associated with Bingham fluids swirling above rotating disk. Rashidi et al. (2013) gave a detailed explanation on the Cu, CuO and Al_2O_3 were the three different nanoparticles considered for analysis above the perforated rotating disks.

The study of ferrofluids forms a basis for producing sustainable energy when the fluid flow is induced over moving objects. The ferrofluid flow with rotating disk on the effect of MHD viscosity and rotation was investigated by Ram and Sharma (2014). Gul et al. (2015) explored the ferroparticles dispersed fluid flowing across a vertical channel accompanied by a magnetic force. The theoretical analysis of Karman swirling flow of mixed convection above a heated rotating disk was done by Guha and Sengupta (2017). An explorative study concerning the flow induced by rotating and vertically moving disk(upward/downward) was given by Turkyilmazoglu (2018). The mixed convective fluid f\/low of hybrid nanomaterial over a heated surface disk was studied by Khan et al. (2019). Bhandari and Husain (2020) investigated the ferrofluid flow in a rotating disc through the mathematical modelling. The problem on stretchable rotating disk with heat transfer of unsteady MHD flow which has dual solution was examined by Sarkar and Sahoo (2021). The viscous flows undergoing

vertical motion subject to heat emitting object and non orthogonal magnetic field is explored by Kumar and Sharma (2023). The computational investigation of axially symmetric flow of magnetite nanofluid is examined by Farooq et al. (2023). A contemporary investigation of fluid flow characteristics with particle swarm optimization with varying thermophysical properties of nanofluid was investigated by Upreti et al. (2023).

The review implies that the flow of ferrofluid subject to low oscillating magnetic field under both a rotating and vertically moving disk is not explored and this problem seems to be possess significant importance in industrial applications. The mathematical equations of axi-symmetric flow of a non-conducting incompressible ferrofluid is formed and are reformed as simultaneous ordinary differential equation by applying similarity transformations and the resultant solutions are attained in Matlab software. The problem is discussed by varying some precised parameters such as volume fraction parameter, disk rotation parameter and expansion/contraction parameter.

2. Mathematical Formulation

Consider the unsteady, laminar, incompressible, electrically non-conducting, nano-ferroliquid flow past an infinite, impermeable disk. The disk is subjected to exhibit both rotational and vertical motion respective to the vertical direction (see Figure 1). Let us assume a non-rotating system of coordinates (r, θ, z) with the respective velocity constituents represented by $(\mathrm{u}, \mathrm{v}, \mathrm{w})$ undergoing an axial symmetric motion. At the starting time $t = 0$, the disk takes the position $a(0) = h$ and the explicit form of $a(t)$is derived in accordance with other pertinent parameters. The time dependent vertical height of the disk from the Origin is expressed as $a(t)$ (at any specific time t), with associated vertical speed of speed is accounted through $\Omega = \dot{a}(t)$. The explicit expression of $a(t)$ is governed by the ancillary flow parameters. The disk rotates around z - axis at a time-dependent rotational speed of $\Omega(t)$. The gravity g is assumed to act along the negative z - direction. The fluid flowing over the rotating surface can be divided into two different regions, the region adjacent to the disk's immediate surface wherein viscous effects are predominant and the outer inviscous region.

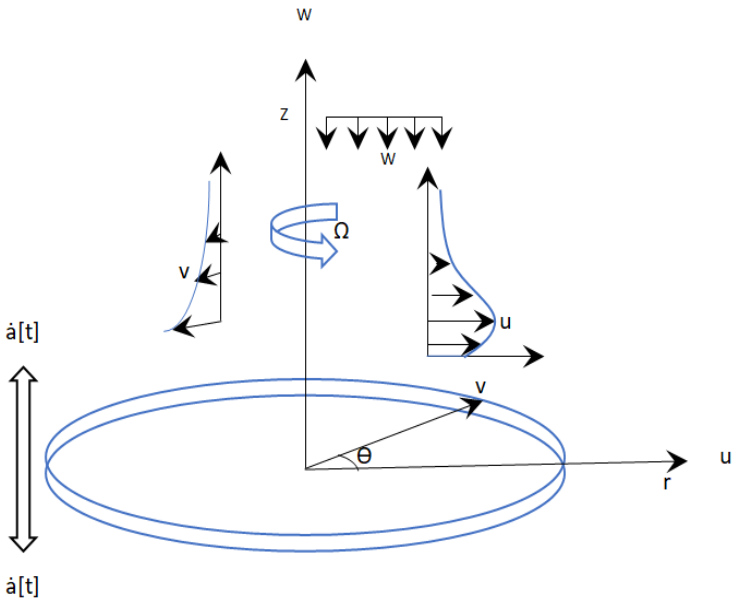

Figure 1. Schematic Configuration of the Flow

Let us assume that T_w governs the disk's temperature at $z = 0$ and the temperature of the ambient fluid is T_∞. In order to achieve positive buoyancy, the temperature of the wall is assumed to be greater than that of the

ambient temperature ($T_w > T_\infty$) which ensures a non-negative temperature difference of $\Delta T = T_w - T_\infty$. The fluid magnetization M in comparison with magnetic field strength $\boldsymbol{H}$ has been described by Langevin parameter and modelled using the Shliomis theory according to Ram and Sharma (2014).

The resultant three dimensional flow with axial symmetric behavior of an incompressible electrically non-conducting ferrofluid takes the mathematical form affirmed with the Boussinesq approximations follows:

$$\frac{\partial u}{\partial r} + \frac{u}{r} + \frac{\partial w}{\partial z} = 0 \quad (1)$$

$$\frac{\partial u}{\partial t} + u\frac{\partial u}{\partial r} + w\frac{\partial u}{\partial z} - \frac{v^2}{r} - \frac{1}{\rho}\frac{\partial p}{\partial r} = \nu\left(1 + \frac{3}{2}\phi M^*\right)\left(\frac{\partial^2 u}{\partial r^2} + \frac{1}{r}\frac{\partial u}{\partial r} + \frac{\partial^2 u}{\partial z^2} - \frac{u}{r^2}\right) + g\beta(T - T_\infty) \quad (2)$$

$$\frac{\partial v}{\partial t} + u\frac{\partial v}{\partial r} + w\frac{\partial v}{\partial z} + \frac{uv}{r} = \nu\left(1 + \frac{3}{2}\phi M^*\right)\left(\frac{\partial^2 v}{\partial r^2} + \frac{1}{r}\frac{\partial v}{\partial r} + \frac{\partial^2 v}{\partial z^2} - \frac{v}{r^2}\right) \quad (3)$$

$$\frac{\partial w}{\partial t} + u\frac{\partial w}{\partial r} + w\frac{\partial w}{\partial z} - \frac{1}{\rho}\frac{\partial p}{\partial z} = \nu\left(1 + \frac{3}{2}\phi M^*\right)\left(\frac{\partial^2 w}{\partial r^2} + \frac{1}{r}\frac{\partial w}{\partial r} + \frac{\partial^2 w}{\partial z^2}\right) \quad (4)$$

$$\frac{\partial T}{\partial r} + u\frac{\partial T}{\partial r} + w\frac{\partial T}{\partial z} = \frac{k}{\rho c_p}\left(\frac{\partial^2 T}{\partial r^2} + \frac{1}{r}\frac{\partial T}{\partial r} + \frac{\partial^2 T}{\partial z^2}\right) \quad (5)$$

The action of wall and quiescent fluid imposed the following boundary conditions:

$$\begin{aligned} z &= a(t): \quad u = 0, \quad v = r\Omega(t), \quad w = \beta\dot{a}(t) \\ z &\to \infty: \quad u \to 0, \quad v \to 0 \end{aligned} \quad (6)$$

In addition, it is noted that $\alpha = 0$ pertains to the constant wall temperature. The wall temperature parameter is taken as 0.5 in this study. The similarity variable η is chosen to satisfy the following velocity variables:

$$u = \frac{r\gamma}{a^2(t)}F(\eta); \qquad v = \frac{r\gamma}{a^2(t)}G(\eta); \qquad w = \frac{\gamma}{a(t)}H(\eta);$$

$$p = \frac{\rho\gamma^2}{a^2(t)}P(\eta); \qquad T = T_\infty + \Delta T\theta; \quad (7)$$

$$\eta = \frac{z}{a(t)} - 1; \qquad \eta_z = \frac{1}{a(t)}; \qquad \eta_t = -\frac{\dot{a}(t)}{a(t)}(\eta + 1)$$

Applying the set of similarity transformations into Eqns.(1) to (5), we obtain the system of similarity transformed mathematical model:

$$2F + H' = 0 \quad (8)$$

$$\left(1 + \frac{3}{2}\phi M^*\right)F'' = F^2 + HF' - G^2 - S\left(\frac{\eta + 1}{2}F' + F\right) - N\theta \quad (9)$$

$$\left(1 + \frac{3}{2}\phi M^*\right)G'' = HG' + 2FG - S\left(\frac{\eta + 1}{2}G' + G\right) \quad (10)$$

$$\left(1 + \frac{3}{2}\phi M^*\right)H'' = P' + HH' + 2FG - \frac{S}{2}((\eta + 1)H' + H) \quad (11)$$

$$\theta'' = PrH\theta' - PrS\left(\frac{\eta + 1}{2}\theta' + \alpha\theta\right) \quad (12)$$

where F, G, H and θ are the dimensionless functions of the modified non-dimensional variable η.

The boundary conditions in view of the set of similarity transformations obtains the form,

$$F(0) = 0; \qquad G(0) = \omega; \qquad H(0) = \beta\frac{S}{2}; \theta(0) = 1$$

$$F(\infty) \to 0; \qquad G(\infty) \to 0; \qquad \theta(\infty) \to 0 \quad (13)$$

where $N = \frac{a^4 g\beta c a^{-2\alpha}}{r\nu^2}$ refers to the mixed convection parameter, Ω is the disk rotation parameter, S is the contraction/extraction parameter, Pr is the Prandtl number, and β represents the permeability parameter in

which $\beta > 1$ refers to flow emission through perforated disk, $\beta < 1$ adheres to flow absorption and $\beta = 1$ governs theimpermeable rigid surface.

The expansion/contraction parameter which denotes the disk movement in vertical direction and the stability of the parameter S is determined by the definition of $a(t)$,

$$a(t) = h\sqrt{1 + t\frac{\gamma S}{h^2}}$$

where the physical parameter Scontrols the upward(>0)/downward(<0) movement of the rotating disk that is expressed through,

$$S = \frac{2a(t)\dot{a}(t)}{\gamma}$$

In addition to this, the disk rotation defines the rate at which the disk exhibits rotational motion which is determined by the angular velocity Ω.. It can be defined as follows:

$$\omega = \frac{\Omega(t)a^2(t)}{\gamma}$$

This implies that$\omega(t) = \frac{\omega\gamma}{h^2+\gamma St}$, which means a decelerating rotating disk for $S > 0$and its an accelerating disk when rotating for $S < 0$ (for finite time). The disk rotation parameter is taken in the range of $1 \leq \omega \leq 3$.

It is accounted that, that the primary parameters of concern are the local skin friction$F'(0)$, $G'(0)$for the coordinatewise drag and torque associated with disk's rotational and vertical movement and the Nusselt number is used to measure the rate of the heat transfer from the rotating disk to the fluid.

3. Numerical Method and Code Validation

The system of differential equations Eqns.(8) to (13) along with its boundary conditions is a simultaneous non-linear differential equations and hence it is difficult to find exact solutions. The Matlab software is used to solve the above problem numerically for different parameter values which is based on finite difference collocation method.

Table 1. Comparison of reduced skin friction values, asymptotic suction velocity and heat transfer coefficient for different S when $\phi = 0$, $\omega = 1$, $\alpha = 0.5$, $M^* = 0$, $N = 0$ and $Pr = 1$ with Turkyilmazoglu (2018).

	S=-0.3		**S=0**		**S=1**	
	Turkyilmazoglu (2018)	**Present**	**Turkyilmazoglu (2018)**	**Present**	**Turkyilmazoglu (2018)**	**Present**
F'(0)	0.4441	0.4437	0.5102	0.5095	0.7523	0.7524
G'(0)	-0.7909	-0.7908	-0.6159	-0.6155	-0.0691	-0.0692
H_∞	-1.0776	-1.09868	-0.8844	-0.8421	-0.1965	-0.1963
-Θ'(0)	0.4968	0.5050	0.3962	0.3991	0.1221	0.1222

Table 2. Comparison of heat transfer coefficient for different S when $\phi = 0$, $\omega = 1$, $\alpha = 0.5$, $M^* = 0$, $N = 0$ and $Pr = 1$ with Turkyilmazoglu (2018).

	α=0		**α=0.2**		**α=0.3**	
	Turkyilmazoglu (2018)	**Present**	**Turkyilmazoglu (2018)**	**Present**	**Turkyilmazoglu (2018)**	**Present**
S=1	0.3308	0.3301	0.1534	0.1524	0.0442	0.0429
S=5	0.2972	0.2973	-0.0716	-0.0716	-0.2989	-0.2990

As the first step, to calculate the solution of the given equations, it requires the starting assumptions which satisfies the boundary conditions. The initial approximation and initial mesh must be provided to the mesh points. Next, the higher order differential equations are converted into first-order differential equations. This provides us a continuous mesh solution. In the computations course, the residual error is usually very small. The solution obtained obeys the set of differential equations at boundaries and interior midpoints.

In order to make sure that the developed codes of the present work are correct, a test was conducted and our results are compared with the previous publication work in the form of table. Table 1 and Table 2 makes a comparative analysis of $F'(0)$, $G'(0)$, $H(\infty)$and $-\theta'(0)$ for differentvalues of S and α among the results of Turkyilmazhoglu (2018) in the absence of both buoyancy and ferro nanoparticles. This clearly shows that there occurs an excellent agreement with the results obtained. These results are obtained by taking $\Omega = 1$, $\mathrm{Pr} = 1$,and $\alpha = 0.5$ with other parameters such as ϕ, M and N as zero in the present work to check the accuracy of the problem and this agrees to the validation of the obtained results.

4. Results and Discussion

The axially symmetric ferrofluid flow and heat transfer of a rigid rotating disk subjected to vertical motion is considered and the corresponding solutions are analyzed for various pertinent parameters. The significant parameters are the volume fraction ϕ of the ferrofluid, the effective magnetization parameter M^*, expansion/contraction parameter S, rotation parameter Ω, buoyancy parameter N, and the Prandtl number Pr. The permeability parameter is fixed as $\beta = 2$ to ensure the impermeability of the disk.

Impact of Disk Rotation and Vertical Motion

Figure 2 explains the behaviour of expansion/contraction parameter S on the radial velocity$F(\eta)$, tangential velocity $G(\eta)$, axial velocity profile $H(\eta)$ and temperature profile $\theta(\eta)$. Figure 2 discusses about $F(\eta)$ for different S wherein the two values (-0.3, -0.2) of S governing the downward disk motion and $S = 0.1, 1$ adheres to upward disk motion. This figure clearly shows that the radial velocity profile like a mounting function and the peaks of radial velocity profile is becoming larger when we increase the parameter nearer the disk's centre and an associated overturn at the latter disk's surface. It is shown that when the disk exerts an upward motion, the radial motion tends to increase. Figure 2b illustrates the impact of expansion /contraction parameter S on the tangential velocity profile. From the figure, we can understand that the fluid tends to move rotationally as a consequence of rotating and upward movement of the disk. In tangential or azimuthal velocity profile, when the speed of the rotating fluid decreases, the boundary layer increases initially and as η takes higher values (or at a distance apart from the origin), an overturn occurs. This prominent velocity increase in the upward motion of the disk causes the fluid in the vicinity of the surface to move upwards which results in this velocity increase. With a keen observation, the diminishing axial velocity is balanced by the tangential velocity as a consequence of the conservation of mass equation Eq.(1).

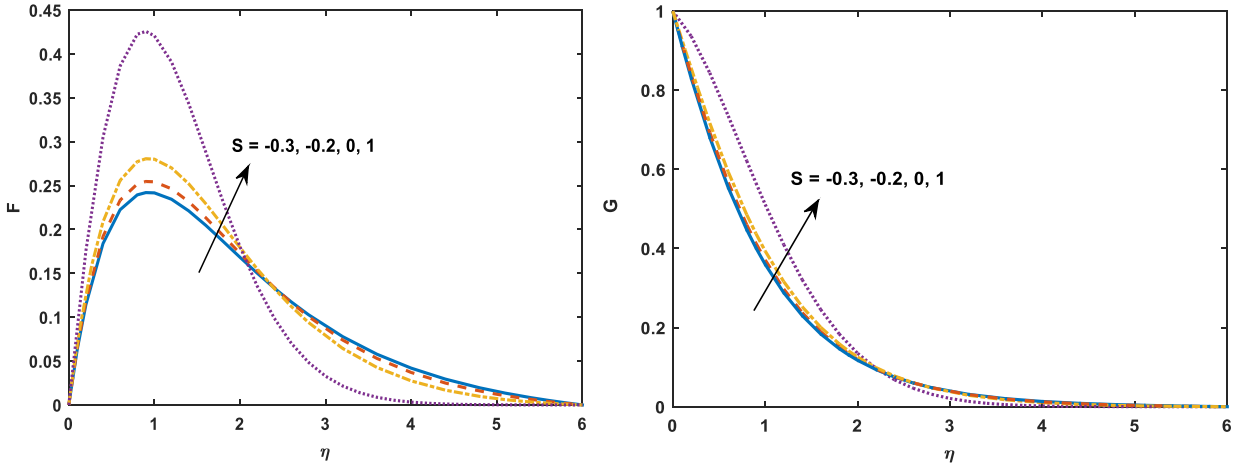

(a) (b)

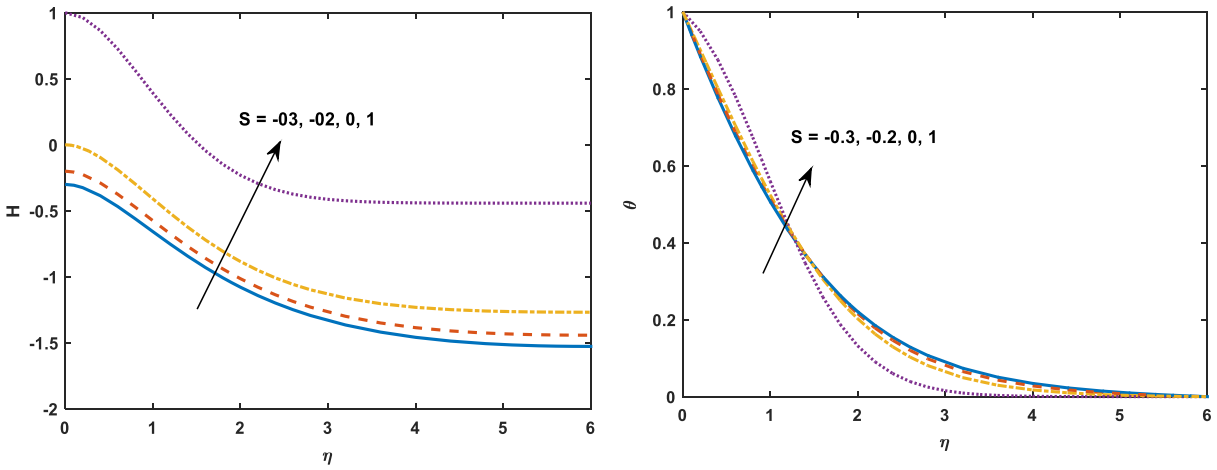

(c) (d)

Fig 2.a,b,c,d: Effect of S on F, G, H, θ when $\alpha = 0.5$, $\omega = 1$, $\phi = 0.05$, $Pr = 1$, $M^* = 0.6$ and $N = 0.5$.

The influence of S on the axial velocity profile is portrayed in Figure 2c. This seems that when $S = 0$, there is no upward/downward movement of the fluid particles in rotating disk, the disk behaves stationary along vertical direction (presuming a von Karman pattern in a ferrofluid). Increasing S shows that the axial velocity profile $H(\eta)$ escalates over the rotating disk in vertical motion. Figure 2d shows the thermal flow behavior with regard to the effect of wall motion S and we observe that the temperature distribution mimics $F(\eta)$ velocity profile. When there is an increase in the parameter S, there is an improvement in the temperature distribution. This is because as S increases, the fluid velocity increases which causes the fluid to get heated up which eventually rises the temperature.

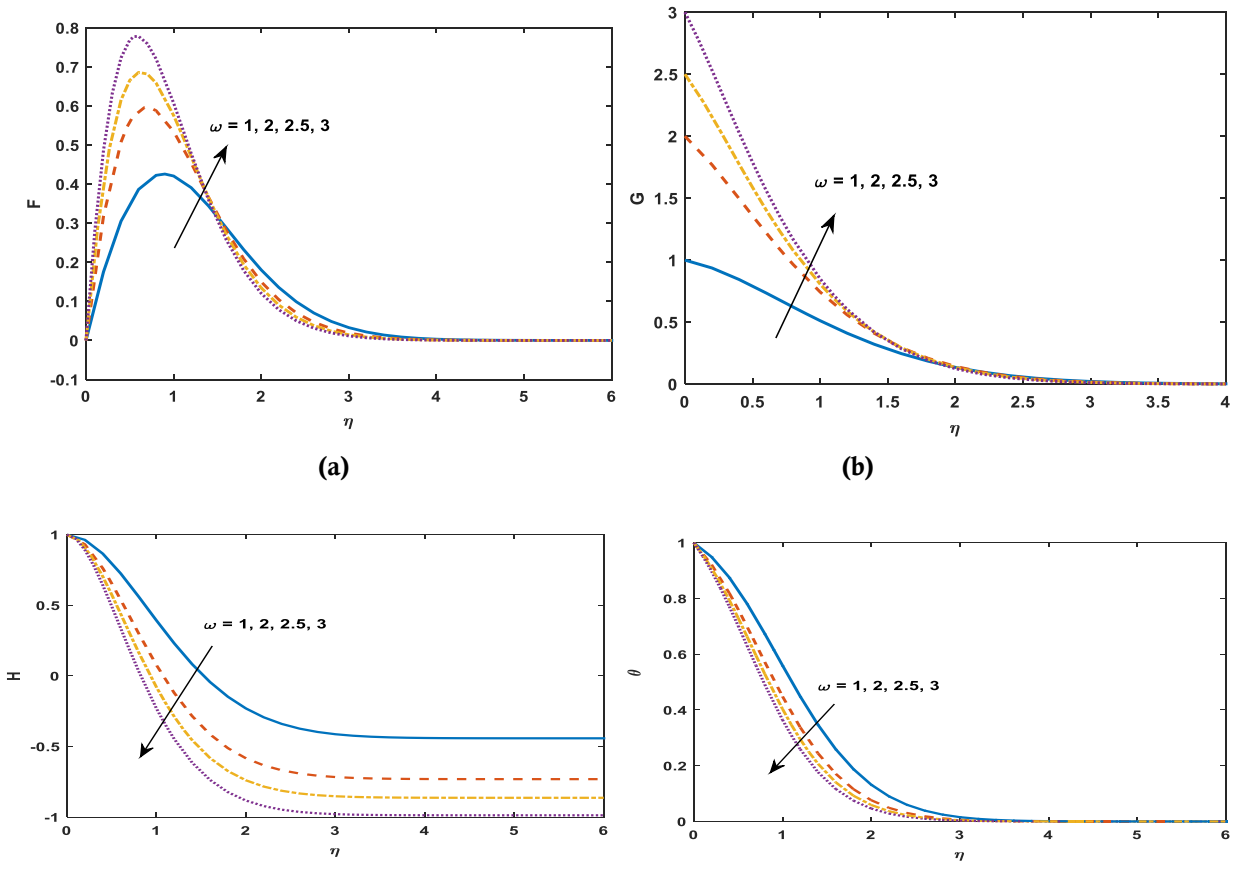

(a) (b)

(c) (d)

Fig 3 a,b,c,d: Effect of ω on F, G, H, θ when $\alpha = 0.5$, $\beta = 2$, $S = 1$, $\phi = 0.05$, $Pr = 1$, $M^* = 0.6$ and $N = 0.5$.

Figure 3 exemplified the impact of the rotation parameter Ωon $F(\eta)$, $G(\eta)$, $H(\eta)$and $\theta(\eta)$. From Figure 3a, we can notice that there is an increase in the rotational speed of the fluid as the parameter Ω increases. This shows that, when we increase the rotation rate, the swirling effect of the fluid particles makes an enhancement in the centrifugal force which imparts a push on the fluid particles radially. After a particular value (approximately $\eta > 1$), Fdecreases gradually as we are away from the disk assuming asymptotic nature. This explains that the effect of centrifugal force is decreasing in the fluid of the disk. The increasing trend of the velocity distribution in tangential direction with an increase in the rotation parameter Ω is presented in Figure 3b. The increase in tangential velocity profile by increasing the parameter Ω is because of the torsional velocity along the tangential direction. This torsional velocity is nothing but an angular velocity which makes the fluid particles to move along the axis of rotation. So, when we increase Ω, tangential velocity profile increases. Figure 3c summarizes the influence of the rotation parameter Ω in fluid movement along the axial direction. This axial velocity profile is a declining function whileincreasing the value of Ω. This happens due to the stronger rotation. As Ω augments, the fluid particles experiences a lateral push radially due to which, a balance is imparted along the negative axial direction. Hence, the enhancement of rotation parameter Ω decreases the velocity distribution in axial direction $H(\eta)$. Figure 3d exhibits the influence of rotation parameterΩ on the temperature profile. This shows that the temperature decreases by increasing the values of Ω. As the fluid is expelled out due to the centrifugal force exerted, the kinetic energy of the fluid is decreased and therefore, the temperature profile $\theta(\eta)$ decreases while increasing the rotation parameter. However the fluid deficit is compensated by the axial velocity of the fluid. Table 3 discusses about three dimensional flow of the problem for the various values of the disk movement. This table clearly shows that the fluid drag due to rotational movement is augmented and asymptotic suction velocity and the limiting value of the average temperature distribution decreases mildly for three dimensional problems.

Table 3. Reduced skin friction values and heat transfer coefficient for different S with ω = 0 when α = 0.5, ϕ = 0.05, M^* = 0.6 ,N = 0.5 and Pr = 1.

ω	S	$F'(0)$	$G'(0)$	H_∞	$-\theta'(0)$
0	-0.2	0.3938	-	-1.3393	0.5083
	0.2	0.4404	-	-0.9616	0.3602
	1.0	0.5378	-	-0.2274	0.0929
	1.5	0.6035	-	0.1961	-0.0574
	2.0	0.6731	-	0.6009	-0.1956
1	-0.2	0.7283	-0.8435	-1.4424	0.5650
	0.2	0.8087	-0.6331	-1.0943	0.4316
	1.0	0.9827	-0.2236	-0.4423	0.1930
	1.5	1.0980	0.0193	-0.0651	0.0591
	2.0	1.2158	0.2502	0.2996	-0.0650

Impact of Ferrofluid

The solid volume fraction of the ferroparticles suspended stably (stable even in huge temperature variations) is taken in the range of $0 \leq \phi \leq 0.1$ and its impact on the ferro-viscous layers over the rotating disk is discussed in Figure 4. Figure 4a shows that the radial velocity profile augments for increasing ϕ values. There is a decrease in the rate of velocity flow after reaching the peak value and it slowly decreases when it comes down for increasing ϕ. Figure 4b illustrates about the tangential velocity profile for increasing the value of volume fraction. The incrementated analysis of solid proportion of ferroparticles clearly affects the flow of fluid in positive manner. When we increase the parameter ϕ, the boundary layer thickness of the fluid decreases and this makes the fluid lighter and makes the fluid to flow easily. So, the velocity profile $G(\eta)$ increases for increasing ϕ value under certain fixed parameters.

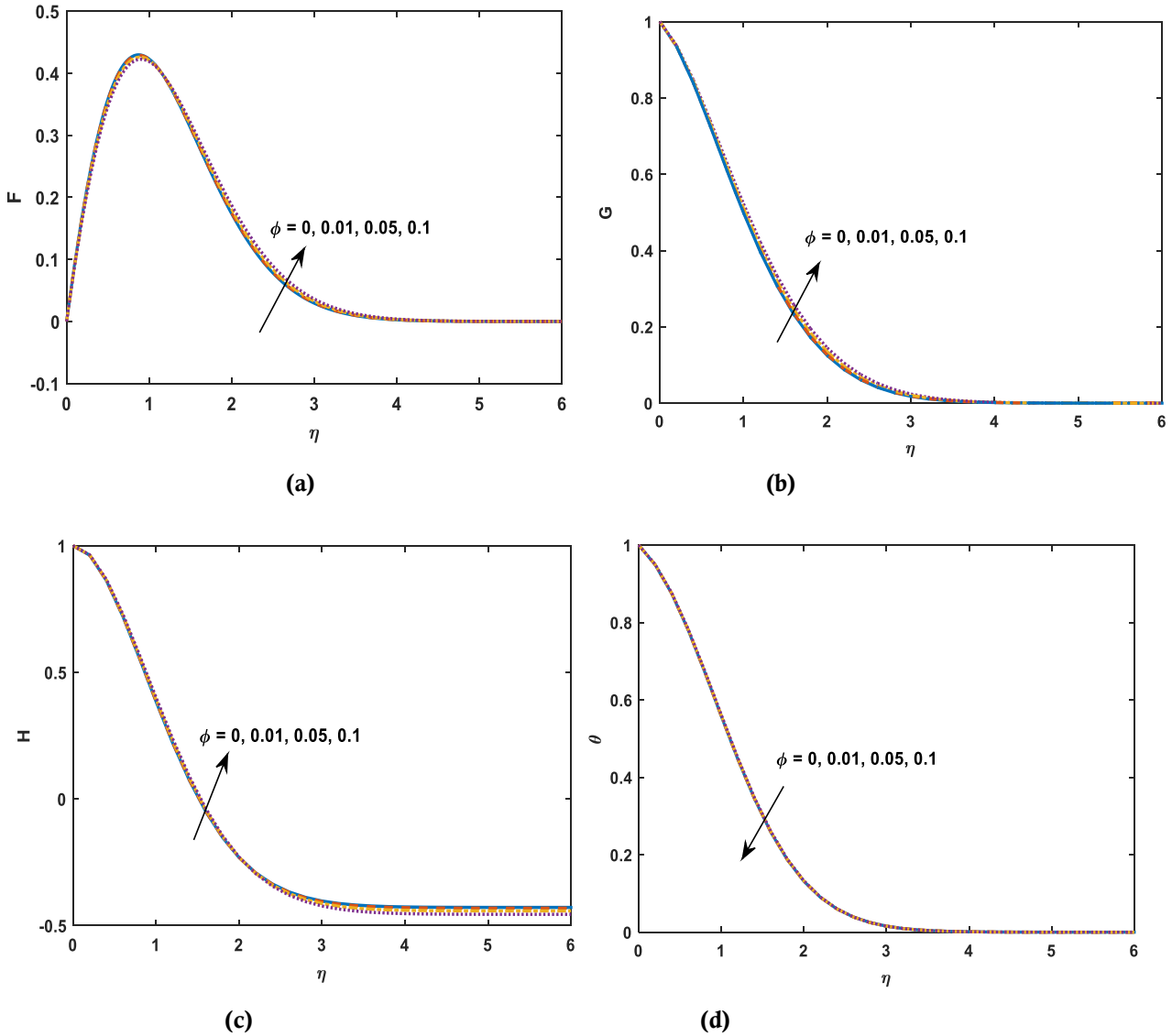

Fig 4 a,b,c,d. Effect of ϕ on θ when $\alpha = 0.5$, $\beta = 2$, $\omega = 1$, $S = 1$, $Pr = 1$, $M^* = 0.6$ and $N = 0.5$.

The demonstration of the effect of volume fraction of the ferrofluid in axial velocity profile is shown in Figure 4c. The figure shows that there is an increase in velocity profile when ϕ value increases and after reaching a particular value it decreases slowly. The increase of ϕ decrease the fluid motion and this happens since the ferrofluid becomes more viscous with increase of ϕ, which decelerates in the motion of fluid flow. Thus the increase of volume fraction in ferrofluid decreases along the vertical direction. The increase of ϕ increments the viscosity of the ferrofluid. Therefore, the axial velocity undergoes retarding effect due to augmented ϕ values. The effect of ϕ on temperature profile is graphically represented in Figure 4d. As we increase the value of volume fraction concentration of ferrofluid, there is a mild decrease in the temperature profile. This shows that there is a slight decrease in the heat absorption in the fluid as the fluid concentration increases. From this, it is clear that the increase in ϕ increases both the electrical and thermal conductivity of the governing fluid, which eventually refrains the thermal boundary layer and improves heat transferring capacity.

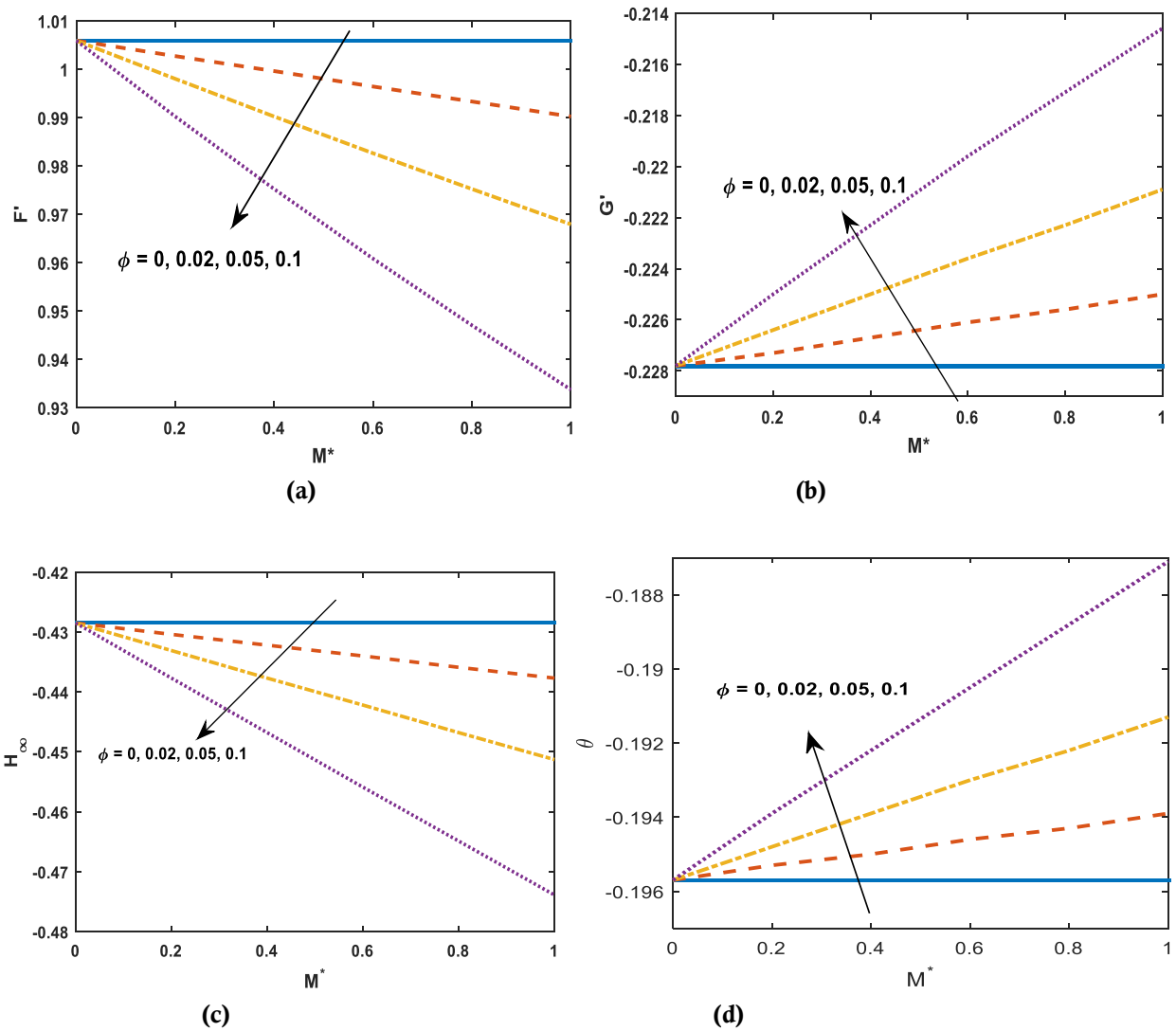

Fig 5 a,b,c,d. Effect of ϕ and M^* on reduced heat transfer coefficient F', G', H', θ' when $\alpha = 0.5, \beta = 2, \quad \omega = 1, S = 1, N = 0.5$ and $Pr = 1$.

The combined effect of the magnetization parameter M^* and the ferroparticle volume fraction ϕ on the reduced skin friction, asymptotic suction profile and the reduced heat transfer coefficient is qualitatively portrayed through the Figure 5. In all the mentioned figures, the strength of magnetization parameter is varied from 0 to 1 and the four different solid volume fractions such as $\phi = 0, 0.02, 0.05, 0.1$ are considered. Figures 5a and 5b displays the influence of ferroparticle volume fraction decreases the reduced skin friction $F'(0)$, along the radial direction and insignificantly increases the reduced skin friction $G'(0)$, along the tangential direction. The result follows from the fact the increase in M^*, increases the resistive force and creates an opposing drag along the radial direction which imparts the reduction in the skin friction values. It can be understood that increasing magnetization parameter M^* decrease the velocity profile in radial direction of ferrofluid. Increasing M^* also enhances the viscosity of ferrofluid, which diminishes the fluid flow in radial direction.

Table 4. Reduced skin friction values and heat transfer coefficient for different ϕ with when ω = 0, S=1, α = 0.5, M^* = 0.6 , N = 0.5 and Pr = 1.

ϕ	0	0.01	0.05	0.1	0.2
$F'(0)$	1.0059	1.0012	0.9827	0.9608	0.9209
$G'(0)$	-0.2278	-0.2270	-0.2236	-0.2196	-0.2121
H_∞	-0.4285	-0.4313	-0.4423	-0.4559	-0.4828
$-\theta'(0)$	0.1957	0.1951	0.1930	0.1905	0.1855

Table 5. Reduced skin friction values and heat transfer coefficient for different withM^* when ω = 1, S = 1, α = 0.5, ϕ = 0.05 , N = 0.5 and Pr = 1.

M^*	0	0.3	0.6	0.9	1
$F'(0)$	1.0059	0.9941	0.9827	0.9716	0.9679
$G'(0)$	-0.2278	-0.2257	-0.2236	-0.2216	-0.2209
H_∞	-0.4285	-0.4354	-0.4423	-0.4491	-0.4513
$-\theta'(0)$	0.1957	0.1943	0.1930	0.1917	0.1913

Table 6. Reduced skin friction values and heat transfer coefficient for different M^* with ω = 0, 1 when α = 0.5, ϕ= 0.05, S = 1, N = 0.5 and Pr = 1.

ω	M^*	$F'(0)$	$G'(0)$	H_∞	$-\theta'(0)$
0	0.0	0.5523	-	-0.2225	0.0971
	0.3	0.5449	-	-0.2249	0.0950
	0.6	0.5378	-	-0.2274	0.0929
	0.9	0.5308	-	-0.2298	0.0908
	1.0	0.5286	-	-0.2306	0.0901
1	0.0	1.0059	-0.2278	-0.4285	0.1957
	0.3	0.9941	-0.2257	-0.4354	0.1943
	0.6	0.9827	-0.2236	-0.4423	0.1930
	0.9	0.9716	-0.2216	-0.4491	0.1917
	1.0	0.9679	-0.2209	-0.4513	0.1913

The asymptotic suction profile H_∞ shown in Figure 5c implies that both M^* and ϕ works together to reduce the fluid transpiration value along the axial direction. The strength of magnetization regulates in regulating the flow nature and hence the formation of viscous layer is retarded with $M^*$and ϕ. The reduced heat transfer coefficient $\theta'(0)$ displayed in Figure 5d reveals that the rate at which thermal transmission occurs is increased effectively by incrementing M^* and ϕ. This is because of the enhanced thermal conductivity of the ferroparticles and the Lorentz force which tends to increase the heat transmission in an enhanced manner. When the value of M^* increases, there is an incrementation in the flow of thermal boundary layer. This creates the presence of viscosity when M^* is increased in ferrofluid. So, the increase of M^* shrinks the vertical velocity distribution H.

The effect of of the radial and tangential skin friction coefficient, asymptotic suction velocity and Nusselt number for varying volume fraction of the ferrofluid is summarized in Table 4. The increase of

ferroparticle concentration increases the tangential skin friction coefficient whereas it declines the radial skin friction coefficient, asymptotic suction velocity and also declines the rate of heat transfer in very small variation when the fluids concentration increases. The result obtained for the effective magnetization on the skin friction coefficients, asymptotic suction velocity and rate of heat transfer is presented in Table 5. It is noticed that the increase of the parameter value only increases the tangential skin friction coefficient, meanwhile it decreases in all other ways. Table 6 signifies the impact of the magnetization parameter $M^*$with disk rotation Ωon the fluid friction values. It was observed that skin friction along the radial direction and the local Nusselt number decreases with M^* and increases with Ω.

5. Conclusion

The ferrofluid flow and associated heat transfer swirling around a non-electrically conducting rotating disk subjective to vertical motion (both upward and downward) are considered. Here, three dimensional flow is introduced when the disk undergoes rotation with imposed low oscillating magnetic field. By adopting some similarity reductions, the transformed governing system of equations have been solved numerically by finite difference collocation based algorithm. The following set of conclusion are made from this study and it can be summarized as follows:

- The increase of nanoparticles in base fluid results in increase of tangential velocity whereas it decreases the velocity profile along both radial and axial direction and affects the thermal profile in a negative way.
- The vertical movement of the disk with its parameter shows an increasing velocity and temperature profile.
- The increased disk rotation enhances the velocity in radial and tangential curves.
- The increase of ferrofluid concentration with respect to the magnetization parameter has an impact on reduced skin friction$G'(0)$along tangential direction and heat transfer coefficient in positive manner.

Acknowledgements

Author P.Gayathri would like to thank PSG College of Arts and Sciences - SEED Fund for the financial support.

References

1. Attia, Hazem Ali, and Ahmed LotfyAboul-Hassan. (2004) .On hydromagnetic flow due to a rotating disk. Applied Mathematical Modelling, 28(12): 1007-1014.
2. Arikoglu,Aytac, and Ibrahim Ozkol. (2006). On the MHD and slip flow over a rotating disk with heat transfer.International Journal of Numerical Methods for Heat& Fluid Flow, 16(2): 172-184.
3. Ahmadpour, Ali, and KayvanSadeghy. (2013): Swirling flow of Bingham fluids above a rotating disk: an exact solution.Journal of Non-Newtonian Fluid Mechanics, 197: 41-47.
4. Bhandari, Anupam, and Akmal Husain, (2020),Unsteady flow and heat transfer of a ferrofluidbetween two rotating, vertical moving and stretching disks.Heat Transfer, 50(2): 1570-1589.
5. Farooq, Umar, Ali Hassan, Nahid Fatima, Muhammad Imran, M. S. Alqurashi, Sobia Noreen, Ali Akgül, and Abdul Bariq, (2023). A computational fluid dynamics analysis on Fe_3O_4–H_2O based nanofluid axisymmetric flow over a rotating disk with heat transfer enhancement. Scientific Reports 13(1): 4679.
6. Guha, Abhijit, and SayantanSengupta. (2017). Non-linear interaction of buoyancy with von Kármán's swirling flow in mixed convection above a heated rotating disc.International Journal of Heat and Mass Transfer, 108: 402-416.
7. Gul, Aaiza, Ilyas Khan, SharidanShafie, Asma Khalid, and Arshad Khan, (2015) Heat transfer in MHD mixed convection flow of a ferrofluid along a vertical channel.PloS one, 10(11): e0141213.
8. Miklavcic, M., and Wang CY, (2004) The flow due to a rough rotating disk.ZeitschriftfürangewandteMathematik und Physik ZAMP, 55: 235-246.
9. Millsaps, Knox, and Karl Pohlhausen, (1952) Heat transfer by laminar flow from a rotating plate. Journal of the Aeronautical Sciences, 19(2): 120-126.

10. Khan, M. Ijaz, Ahmed Alsaedi, Tasawar Hayat, and Niaz B. Khan, (2019). Modeling and computational analysis of hybrid class nanomaterialssubject to entropy generation. Computer Methods and Programs in Biomedicine, 179: 104973.
11. Kumar, Sanjay, and Kushal Sharma. (2023). Entropy optimization analysis of Marangoni convective flow over a rotating disk moving vertically with an inclined magnetic field and nonuniform heat source.Heat Transfer 52.2: 1778-1805.
12. Sarkar, G. M., and Sahoo B, (2021). On dual solutions of the unsteady MHD flow on a stretchable rotating disk with heat transfer and a linear temporal stability analysis." European Journal of Mechanics-B/Fluids, 85: 149-157.
13. Ram, Paras, and Kushal Sharma. (2014). Effect of rotation and MFD viscosity on ferrofluid flow with rotating disk. Indian Journal of Pure and Applied Physics, 52: 87 -92.
14. Rashidi, M. M., S. Abelman, and N. FreidooniMehr. (2013). Entropy generation in steady MHD flow due to a rotating porous disk in a nanofluid. International journal of Heat and Mass transfer, 62: 515-525.
15. Turkyilmazoglu, Mustafa, (2018). Fluid flow and heat transfer over a rotating and vertically moving disk.Physics of Fluids, 30(6):063605.
16. Upreti, Himanshu, ZiyaUddin, Alok Kumar Pandey, and Navneet Joshi, (2023) Particle swarm optimization based numerical study for pressure, flow, and heat transfer over a rotating disk with temperature dependent nanofluid properties." Numerical Heat Transfer, Part A: Applications, 83(8): 815-844.